Journal of Hazardous Materials 177 (2010) 508–515

Contents lists available at ScienceDirect

Journal of Hazardous Materials

journal homepage: www.elsevier.com/locate/jhazmat

Enrichment of chlorobenzene and *o*-nitrochlorobenzene on biomimetic adsorbent prepared by poly-3-hydroxybutyrate (PHB)

Xiaoxuan Zhang[a], Chaohai Wei[a,b,*], Qincong He[b], Yuan Ren[b]

[a] College of Chemistry and Chemical Engineering, South China University of Technology, Guangzhou 510640, PR China
[b] College of Environmental Science and Engineering, South China University of Technology, Guangzhou 510006, PR China

ARTICLE INFO

Article history:
Received 15 May 2009
Received in revised form
12 December 2009
Accepted 14 December 2009
Available online 21 December 2009

Keywords:
Enrichment
Biomimetic adsorbent
Poly-3-hydroxybutyrate (PHB)
Chlorobenzene
o-Nitrochlorobenzene

ABSTRACT

Poly-3-hydroxybutyrate (PHB) was used as a new material to prepare a biomimetic adsorbent by a modified double emulsion solvent evaporation technique. The enrichment capacities of the adsorbent for the toxic liposoluble organic compounds were evaluated by chlorobenzene (CB) and *o*-nitrochlorobenzene (*o*-NCB) with the adsorption isotherms, enrichment factor (EF) and enrichment kinetics. The results showed that Sips isotherm fitted the experimental data better than Langmuir and Freundlich models, as well as the pseudo-second order kinetic model fitted better than the first order model. For CB and *o*-NCB, the maximum adsorption capacity was 125.99 and 39.56 mg g^{-1}, while the maximum EF was 1204 and 1149 at 20 °C for 36 h, though the specific surface area (BET) of the adsorbent was only 8.45 m^2 g^{-1}. CB had a higher EF than *o*-NCB because the hydrophilic group ($-NO_2$) decreases the liposoluble ability of *o*-NCB. K_{ow} has a positive correlation with EF, so the organochlorine compounds are liable to be adsorbed by the adsorbent. The results indicated that PHB, even polyhydroxyalkanoates, can be a new biodegradable adsorption material.

1. Introduction

The pollution of organochlorine compounds (OClCs) including chlorinated aliphatic, alicyclic, aromatic, polycyclic aromatic hydrocarbons and their derivatives are of great concern owing to their carcinogenic, teratogenic and mutagenic effects [1]. OClCs mainly have three sources: industrial and agricultural discharges, chlorine disinfection by-products (DBPs) of drinking water and wastewater, and incineration of wastes. The chlor-alkali industry is a main source of chlorine, and OClCs such as chlorobenzene (CB) and nitrochlorobenzene (NCB) [2–4]. China is a large producer of chlorine and pesticides. The production of chlorine was about 13.74 million tons in 2006 [2], and that of hexachlorobenzene (HCH) and dichlorodiphenyltrichloroethane (DDT) were 4.9 and 0.4 million tons, respectively, during 1950–1983 accounting for 33% and 20% of the total production in the world [5,6]. Many OClCs had been detected in the effluents from the municipal wastewater plant and wastewater treatment factory, which were DBPs (disinfection by-products) and industry discharge [7–11]. In incineration processes, HCH and polychlorinated dibenzo-*p*-dioxins and dibenzofurans (PCDD/F) could be converted by other low toxicity compounds [12].

Although the total amount of OClCs in the environment is large, their concentrations in natural waters are very low. A survey on seven rivers in China (Songhuajiang River, Liaohe River, Haihe River, Yellow River, Yangtze River, Huaihe River and Pearl River) showed that the concentrations of γ-HCH, *p*,*p*′-DDT and heptachlor epoxide were 0.17–860, 0.14–368, 0.11–10 ng L^{-1}, respectively, and that of NCBs were 0.01–5.072 μg L^{-1} [13,14]. It has been reported that many aerobic and anaerobic microorganisms can degrade OClCs [15–18], though it is quite time-consuming. For example, it took 202–230 h for biodegradation of 80–90% of 1,4-dichlorobenzene (132 mg L^{-1}) by two pure aerobic bacterial cultures [18]. Thermodynamically, biodegradation of OClCs is feasible, while due to their low degradation rates and low aqueous concentrations, OClCs are kinetically limited, leading to difficult applications in engineering. An effective alternative for eliminating OClCs is the utilization of advanced oxidation processes [19], while the equipment limitation in treating large amount of wastewater at extremely low levels of OClCs limits its engineering applications. Therefore, there is a great demand for developing effective methods to enhance aqueous concentration of OClCs.

Based on their hydrophobic nature, lipophilic OClCs are liable to bioaccumulation in organisms containing abundant lipid, such as zooplankton, fish, seal and waterbird [20–23]. The accumulation level of a contaminant can be assessed by BCF (bioconcentra-

* Corresponding author at: College of Environmental Science and Engineering, South China University of Technology, Guangzhou 510006, PR China.
Tel.: +86 20 39380588; fax: +86 20 39380588.
E-mail address: cechwei@scut.edu.cn (C. Wei).

0304-3894/$ – see front matter © 2009 Elsevier B.V. All rights reserved.
doi:10.1016/j.jhazmat.2009.12.062

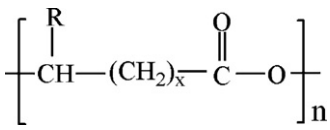

Fig. 1. Structure of PHAs (PHB, while $x = 1$ and R is methyl group).

tion factor), which is a dimensionless ratio of the concentration of a contaminant in the organism to that in the water. BCF_{lipid} (based on lipid content) of 13 OCPs in 18 fish species ranged 1000–251,189, and the bioaccumulation capacity of fish organs was in the order of brain > kidney > liver > heart > muscle [22]. All these show that OClCs easily accumulate in lipid phase. We predict that the ester/lipid of organisms can transfer OClCs from water, so polyhydroxyalkanoates (PHAs) may enrich OClCs. PHAs are biodegradable polyesters [24], which contain the same functional groups of the lipid, such as the ester group and hydrocarbyl. PHAs are produced by many bacteria and other microorganisms through degrading wastes and contaminants under unbalanced growth conditions [25–27] and their structure is shown in Fig. 1, where R is hydrocarbyl. Poly-3-hydroxybutyrate (PHB), a representative compound of PHAs, has been extensively studied and used as tissue engineering materials due to its biocompatibility [24,25]. Therefore, we suppose that PHB can be used as an adsorption material to accumulate OClCs from water by phase transfer though it has not been reported.

Bionics is a multidisciplinary science that researches the principles, properties and mechanisms of natural systems such as structures, processes, functions, organizations and interrelations to apply them in the development of new products or solving technical problems that may arise during project-phase [28]. We know that fish can accumulate OClCs by a balance process between uptake and depuration [29], because OClCs are hardly degradable and readily dissolved in lipid. According to the bionics principles, we could prepare an adsorbent used PHB to realize the accumulation process. Adsorption of OClCs on the porous adsorbent was regarded as an uptake process of fish, and PHB was like the lipid with strong affinity for organic pollutants. The saturated adsorbent and adsorbed pollutants could be degraded by supercritical water reduction/oxidation for dechlorination and hydrogen generation [30,31].

In this study, PHB was used to prepare a biomimetic adsorbent named as PHBBMA. To evaluate the adsorption/enrichment capacity of PHBBMA, CB and *o*-NCB were chosen since their structure is compared conveniently and they are always released to the environment during manufacturing and application processes as carrier, solvent and/or intermediate [18,32]. PHBBMA was characterized by the scanning electron microscopy (SEM), specific surface area (BET) and pore size distributions, and its enrichment properties were described with adsorption isotherms, enrichment effect and enrichment kinetics at different temperatures. The research conclusions provide evidence for a new safe and environment friendly pollution control method of the toxic OClCs.

2. Experimental

2.1. Chemicals

PHB was obtained from Sigma–Aldrich Co. (St. Louis, MO, USA), and its T_m is 172 °C. Polyvinyl alcohol (PVA) and chloroform were purchased from Guangdong Guanghua Chemical Factory Co. (Guangzhou, China). Analytical standard CB and *o*-NCB were purchased from Sigma–Aldrich Co., which characteristics are summarized in Table 1.

2.2. PHBBMA preparation

The monomer polymerization is a common method of preparation of organic polymer adsorbent, which always includes a series of complex process with strict reaction conditions [34–36]. The toxicity of pore forming agents and the long preparation period are its disadvantages. So in this paper, we used a modified double emulsion water-in-oil-in-water ($W_1/O/W_2$) solvent evaporation technique to prepare PHBBMA. The solvent evaporation technique is always used to encapsulate drugs, and W_1 is water solution containing drug [37]. The simple and low cost method is borrowed to prepare adsorbent, and deionized water was instead of drug solution to be as pore forming agent. After preliminary experiments, the preparation conditions were selected as follows: 12 mL of deionized water was dropped into 30 mL of chloroform solution containing 3% (w/w) PHB, evenly mixed with a homogenizer at a stirring rate of 10,000 r min^{-1} for 2 min at 25 °C to obtain the primary W_1/O emulsion. The primary emulsion was then injected into and mixed with 200 mL of aqueous solution containing 3% (w/w) PVA at 800 r min^{-1} for 4 min to form the $W_1/O/W_2$ double emulsion. The double emulsion was diluted with 200 mL of deionized water, and stirred at 500 r min^{-1} for 36 h to evaporate the chloroform and solidify PHBBMA. PHBBMA particles were filtered, washed with deionized water and freeze-dried.

2.3. Adsorption/enrichment experiments

Adsorption/enrichment process was affected by temperature, so according to the actual temperature of wastewater at different conditions, the adsorption experiments were did at 20, 30 and 40 °C, respectively. CB and *o*-NCB were adsorbed respectively by PHBBMA with a batch method to reveal the effect of hydrophilic group on adsorption/enrichment. A dose of 100 mg of PHBBMA was added into 100 mL of CB or *o*-NCB aqueous solution in a 150-mL conical flask, sealed with a stopper, and stirred at 200 r min^{-1} under the constant temperatures, while blank test was arranged. All the experiments were conducted in triplicate, and the mean values have been reported. Considered to aqueous

Table 1
The characteristics of CB and *o*-NCB.

Chemicals (abbreviation)	CAS number	Structure	Molecular weight	Log K_{ow}[a]	S_w[b] at 25 °C (mg L^{-1})
Chlorobenzene (CB)	108-90-7	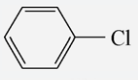	112.56	2.84	498
o-Nitrochlorobenzene (*o*-NCB)	88-73-3	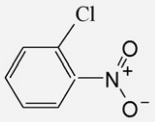	157.56	2.24	441

[a] Octanol/water partition coefficient.
[b] Aqueous solubility, [a,b]Source [33].

solubility of CB and *o*-NCB, and based on preliminary study, the initial concentration ranges were set from 0.56 to 131.04 mg L^{-1} (4.99×10^{-3} to 1.16 mmol L^{-1}) for CB and from 0.98 to 97.55 mg L^{-1} (6.19×10^{-3} to 0.62 mmol L^{-1}) for *o*-NCB to determine adsorption isotherms and enrichment effect. The equilibrium time was 36 h, which was determined by preliminary study. The kinetics was studied at initial concentration of 0.56, 5.62 and 37.44 mg L^{-1} (4.99×10^{-3}, 4.99×10^{-2} and 0.32 mmol L^{-1}) for CB, and of 0.98, 9.76 and 54.63 mg L^{-1} (6.19×10^{-3}, 6.19×10^{-2} and 0.35 mmol L^{-1}) for *o*-NCB. The concentration of adsorbate on PHBBMA, q (mg g^{-1}), was calculated by the equation:

$$q = \frac{(c_0 - c)V}{m} \quad (1)$$

where c_0 (mg L^{-1}) and c (mg L^{-1}) are the concentrations of adsorbate in the solution at time 0 and t (h), respectively. V (L) is the solution volume, and m (g) is the dose of adsorbent.

Enrichment factor (EF) was used to evaluate the accumulation ability of PHBBMA, which borrowed the definition from BCF [29]. EF is distinguished from BCF which illuminates the concentration capacity of living organisms:

$$EF = \frac{q_e \rho}{c_e} \quad (2)$$

where q_e (mg g^{-1}) and c_e (mg L^{-1}) are the concentrations of adsorbate on PHBBMA and in the solution at equilibrium, respectively. ρ, solution density, is about 1000 g L^{-1}. The enrichment capacity of PHBBMA should be positively correlated with EF.

2.4. Analytical methods

The shapes and surface morphology of PHBBMA were investigated by JSM-6300F SEM of JEOL Ltd. (Tokyo, Japan). Samples were dried overnight and sputter coated with gold prior to imaging. The specific surface area and pore distribution were measured by ASAP 2010M from Micromeritics (Norcross, GA, USA) with the BET (Brunauer–Emmett–Teller) and BJH (Barrett–Joyner–Halenda) methods through N_2 adsorption at 77 K [38].

CB and *o*-NCB concentrations were determined by LC-20A high performance liquid chromatography (HPLC) purchased from Shimadzu (Kyoto, Japan) with external standard method. Samples were separated using an Agilent HC-C18 column (4.6 mm × 250 mm) (Santa Clara, CA, USA) at 40 °C and detected by UV detector at 254 nm. The mobile phase was methanol/water (70/30, v/v) at a flow rate of 1.000 mL min^{-1}, and sample injection volume was 10 μL for 18 min of the retention time. Samples were filtered through a 0.45 μm syringe filter prior to injection into HPLC column. The minimum detection limit (MDL) of HPLC as the compound concentration at a signal-to-noise ratio of 3. The MDL values of CB and *o*-NCB were 0.08 and 0.06 mg L^{-1}, respectively. The calibration curves were established by injecting six standard solutions, ranging from 0.53 to 106.6 mg L^{-1} (4.74×10^{-3} to 0.95 mmol L^{-1}) for CB with the linear fitting coefficient (R) of 0.9998, and ranging from 0.52 to 104.3 mg L^{-1} (3.31×10^{-3} to 0.66 mmol L^{-1}) for *o*-NCB with R of 0.9999.

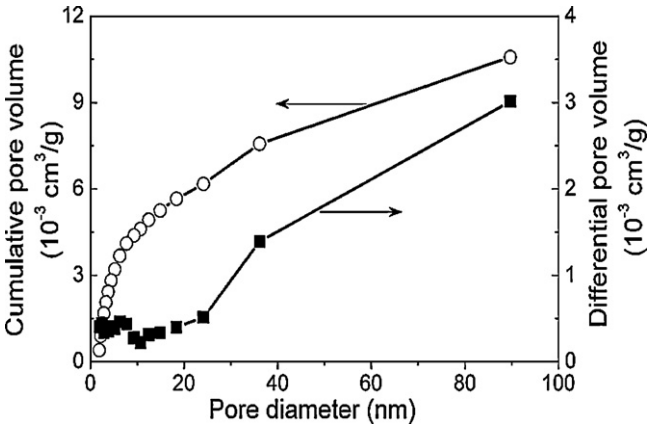

Fig. 3. Pore size distributions of PHBBMA.

3. Results and discussion

3.1. Properties of PHBBMA

The textural and surface characteristics of PHBBMA are shown in Fig. 2. The results indicated that PHBBMA was spherical particles with rough surface and micropores. The diameter of most PHBBMA particles was 100–200 μm. The BET surface area, total pore volume, and average pore diameter were 8.45 m^2 g^{-1}, 0.0105 cm^3 g^{-1}, and 4.9 nm, respectively. Fig. 3 describes the cumulative and differential pore volume of PHBBMA with the pore diameter range of 1.9–89.7 nm. According to the definition by IUPAC, the adsorbent pores are classified into three groups: micro-pore (diameter < 2 nm), meso-pore (2–50 nm), and macro-pore (>50 nm), so the main pores of PHBBMA were meso- and macro-pores. The pores were produced by the vaporization of chloroform solvent and water (W_1), so the pore diameter was determined by the concentration of PHB in chloroform and the diameter of water particles. In this study, the water particle sizes were large due to the limitation of stirring speed of homogenizer, i.e., the pore diameter was large and the specific surface area was small.

The adsorption capacity of adsorbent is related to specific surface area and affinity between the adsorbent and adsorbate. Due to the specific surface area of PHBBMA being limited by the apparatus,

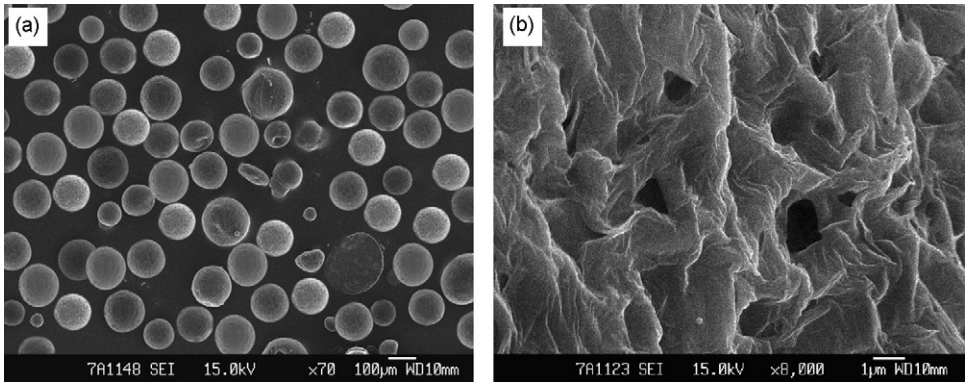

Fig. 2. Scanning electron micrographs of PHBBMA: (a) whole particles × 70 and (b) surface of particle × 8000.

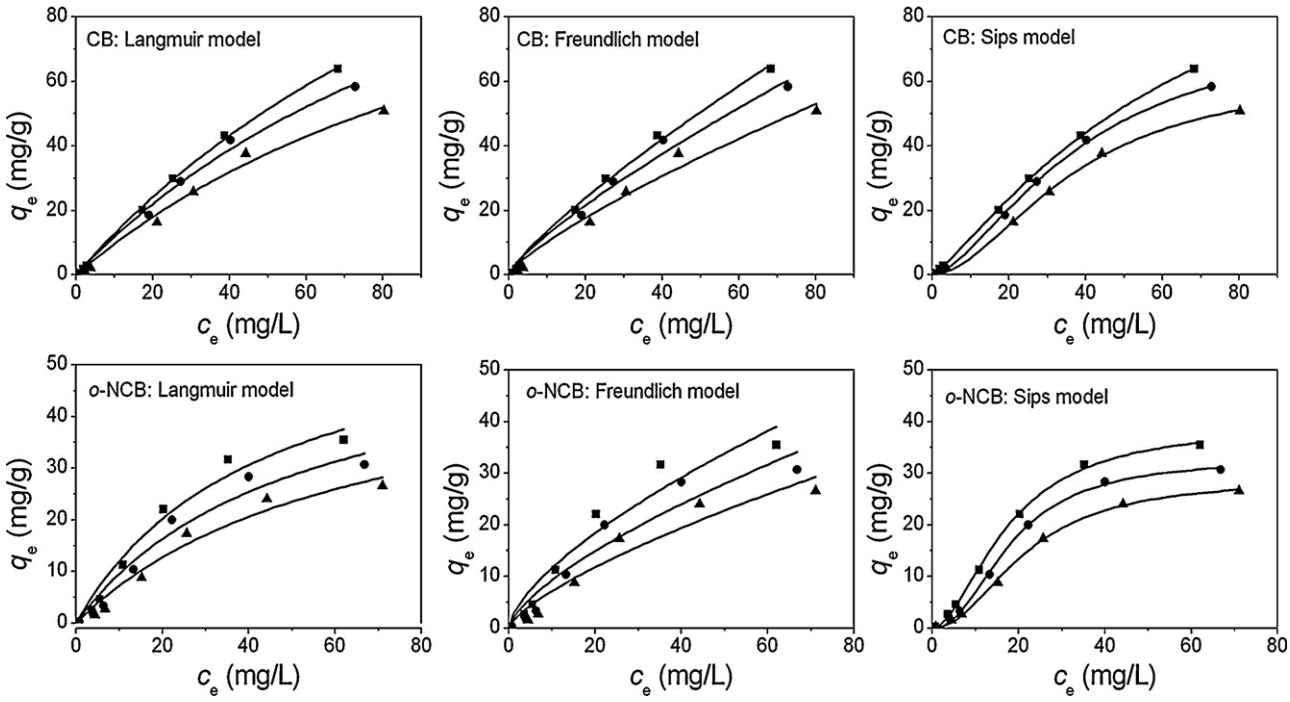

Fig. 4. Adsorption isotherms of CB and *o*-NCB on PHBBMA: experimental data at 20 °C (■), 30 °C (●) and 40 °C (▲); isotherm models fitting (—).

the affinity plays an important role, so two adsorbates, CB and *o*-NCB, were used to evaluate the adsorption ability of PHBBMA. The meso- and macro-pores of PHBBMA were favorable for the adsorption of CB and *o*-NCB, since water was easy to penetrate in these pores, and the collision probability of chemicals with PHBBMA increased. If the adsorption ability is proved, the further study will be reported in other paper. For example, the preparation conditions will be optimized, and other pore foaming agents will be tried. Activated carbon and molecular sieve may be as carriers to increase the surface area of PHBBMA.

3.2. Adsorption isotherms

Analysis of sample blanks indicated that there was not significant loss of CB and *o*-NCB over the test duration. The adsorption tests were carried out and the adsorption isotherms of CB and *o*-NCB in aqueous solutions onto PHBBMA are shown in Fig. 4. The experimental data were analyzed using Langmuir, Freundlich and Sips models, and their parameters are presented in Table 2. The Langmuir isotherm can be represented as [39,40]:

$$q_e = \frac{q_m b_L c_e}{1 + b_L c_e} \quad (3)$$

where q_m (mg g^{-1}) and b_L (L mg^{-1}) are constants related to adsorption capacity and energy of adsorption, respectively. The Langmuir equation is used for homogeneous surfaces. Though the values of R^2 (0.967–0.999) expressed in Table 2 were high, Fig. 4 shows that Langmuir was not available to fit the experimental data.

The Freundlich isotherm is given as [38,40–41]:

$$q_e = K_F c_e^{1/n} \quad (4)$$

where K_F [mg$^{(1-1/n)}$ L$^{1/n}$ g^{-1}] and n are constants. The Freundlich isotherm originally was an empirical equation, but has been later interpreted in theory. K_F and n are indicators of adsorption capacity and intensity, respectively. The Freundlich model showed a higher extent of deviation from the data compared to the other models in both systems since the R^2 values of the Freundlich model were lower than that of the other models (Table 2). The result was also proved in Fig. 4.

The Sips isotherm, which always describes the adsorption of the adsorbent with heterogeneous surface, is a three-parameter equation. Sips equation similar in form to the Freundlich equation, but it has a finite limit when the concentration is sufficiently high [40,42]:

$$q_e = \frac{q_m b_S c_e^{\gamma}}{1 + b_S c_e^{\gamma}} \quad (5)$$

Table 2
Adsorption isotherm parameters for CB and *o*-NCB on PHBBMA.

Chemical	T (°C)	Langmuir model			Freundlich model			Sips model			
		q_m	$b_L \times 10^3$	R^2	K_F	$1/n$	R^2	q_m	$b_S \times 10^3$	γ	R^2
CB	20	208.60 (19.56)[a]	6.52 (0.81)	0.999	2.04 (0.29)	0.82 (0.04)	0.996	125.99 (7.04)	6.07 (0.34)	1.22 (0.04)	1.000
	30	165.91 (29.65)	7.63 (1.90)	0.995	1.99 (0.48)	0.80 (0.06)	0.990	80.31 (6.03)	2.89 (1.05)	1.59 (0.14)	0.999
	40	140.69 (31.57)	7.31 (2.31)	0.992	1.64 (0.49)	0.79 (0.07)	0.984	63.20 (3.86)	1.25 (0.67)	1.85 (0.18)	0.999
o-NCB	20	63.48 (10.76)	23.28 (7.32)	0.978	2.52 (0.93)	0.66 (0.10)	0.950	39.56 (1.17)	5.57 (1.39)	1.81 (0.11)	0.999
	30	57.83 (13.10)	19.59 (7.98)	0.967	1.91 (0.84)	0.69 (0.11)	0.938	32.89 (0.74)	1.77 (0.59)	2.18 (0.13)	0.999
	40	53.99 (13.07)	15.39 (6.34)	0.972	1.37 (0.60)	0.72 (0.11)	0.949	29.01 (0.80)	1.59 (0.58)	2.10 (0.13)	0.999

[a] The standard error of the fitting value of the parameters.

where q_m (mg g^{-1}) is the maximum adsorption capacity, b_S (L$^{\gamma}$ mg$^{-\gamma}$) is a constant related to adsorption energy, and γ is the Sips exponent. The Sips model fitted experimental data well, as indicated in both Fig. 4 and Table 2 ($R^2 > 0.999$).

Fig. 4 shows that the adsorption amount of CB was always greater than that of *o*-NCB in the same conditions, and the adsorption capacity decreased when the temperature increased for both CB and *o*-NCB. The results were also expressed by q_m values of the Sips equation in Table 2. It was because that adsorption capacity was positive correlation with the affinity between PHBBMA and chemicals, and CB had more strong affinity than *o*-NCB due to absence of $-NO_2$. The adsorption capacity had a negative effect on the temperature because the octanol–water partition coefficient (K_{ow}) decreased and aqueous solubility increased with the temperature increasing for CB [43]. That is the affinity between CB and PHBBMA decreased when the temperature increased. The effect of temperature on *o*-NCB could be explained with the same reason. These meant that PHBBMA could adsorb CB and *o*-NCB well. The q_m was 125.99, 80.31 and 63.20 mg g^{-1} for CB, and 39.56, 32.89 and 29.01 mg g^{-1} for *o*-NCB at 20, 30 and 40 °C, respectively, under experimental conditions.

Table 2 shows that q_m of CB on PHBBMA was 165.91 mg g^{-1} according to Langmuir model at 30 °C, but q_m in unit surface area was 19.6 mg m^{-2} since its surface area was only 8.45 m^2 g^{-1}. Sennour et al. reported that q_m of CB on activated montmorillonite with BET surface area of 250 m^2 g^{-1} was 174.8 mg g^{-1} according to Langmuir model at 28 °C, but q_m in unit surface area was only 0.7 mg m^{-2} [43]. The result showed that PHBBMA had a potential advantage and could increase adsorption capacity through increasing surface area.

3.3. Enrichment ability of PHBBMA

Enrichment ability of PHBBMA was an important parameter, so EF was defined as a criterion. EF of PHBBMA for CB and *o*-NCB were calculated using the experimental equilibrium data and Sips equation fitting data, respectively. The variety of EF with equilibrium concentration is shown in Fig. 5. For both chemicals, EF increased at first and then decreased when the equilibrium concentration increased. Under low concentrations, PHBBMA had enough available sites, so q_e could increase faster than c_e (Fig. 4), which indicates that EF increased with the increase of c_e. Under high concentrations, adsorbent was gradually saturated, causing q_e increased slowly, even kept constant, so EF decreased with the increase of c_e. EF for CB and *o*-NCB had the same trends, with $EF_{20\,°C}$ (EF at 20 °C) > $EF_{30\,°C}$ > $EF_{40\,°C}$. This was because when temperature increased, K_{ow} decreased and aqueous solubility increased for CB [44]. High K_{ow} and low aqueous solubility imply strong lipophilic and hydrophobic properties, which causes the easy adsorption of CB on PHBBMA. The same reason could be considered for *o*-NCB. Fig. 5 also shows that EF values calculated by the Sips fitting data were consistent with the experimental results at high equilibrium concentrations, but a great difference existed at very low concentrations. This is because the high concentration would conceal the variety at low concentration when the simulation data were calculated with the same equation, and the measurement error was bigger at low c_e than at high c_e. It indicates that the Sips model may not fit the experimental data well at low concentrations, but it could be used to accurately predict EF at $c_e > 30$ mg L^{-1} for CB and $c_e > 25$ mg L^{-1} for *o*-NCB. This also showed that the simulation could accurately predict EF at low concentrations when the adsorption isotherm fitted the experimental data well.

PHBBMA had higher enrichment capacity for CB than for *o*-NCB because the former had higher K_{ow} than the latter (Table 1). Though a small aqueous solubility is always in favor of the adsorption process, it is not suitable for CB and *o*-NCB. Because that *o*-NCB is solid at normal temperature, and its aqueous solubility is related to its crystal lattice energy, while adsorption capacity is influenced by hydrophobic property [38]. Therefore, their difference of EF cannot be explained by the different solubility, and should be determined by K_{ow}. The hydrophilic group, $-NO_2$, increases the hydrophilicity of *o*-NCB, so PHBBMA has better adsorption affinity for CB than for *o*-NCB. The maximum EF were 1204, 1064 and 860 for CB, and 1149, 916 and 689 for *o*-NCB at 20, 30 and 40 °C for 36 h, respectively. The results showed that PHBBMA has a good enrichment effect for CB and *o*-NCB, and PHB is a suitable adsorption material for OClCs. It can predict that OClCs with higher K_{ow} will have higher EF than CB and *o*-NCB. In the future, the mathematical relation between K_{ow} and EF will be constructed to predict enrichment effect with chemical structure.

3.4. Enrichment/adsorption kinetics

The enrichment rate is one of the key factors of the practical application, so the kinetics was studied. The rate law is always determined by experimentation, but it cannot be inferred by more examination of the overall chemical reaction equation because the solid-solution adsorption process is complex [45]. The pseudo-first and -second order models were based on solution concentration for the sorption of chemicals from liquid phase onto solid adsorbent, as a reversible reaction with an equilibrium being established between two liquid and solid phases [45]. So the two models are always used to express the mechanism of adsorption in liquid–solid systems. The former is expressed as [40,45]:

$$\frac{dq}{dt} = k_1(q_e - q) \quad (6)$$

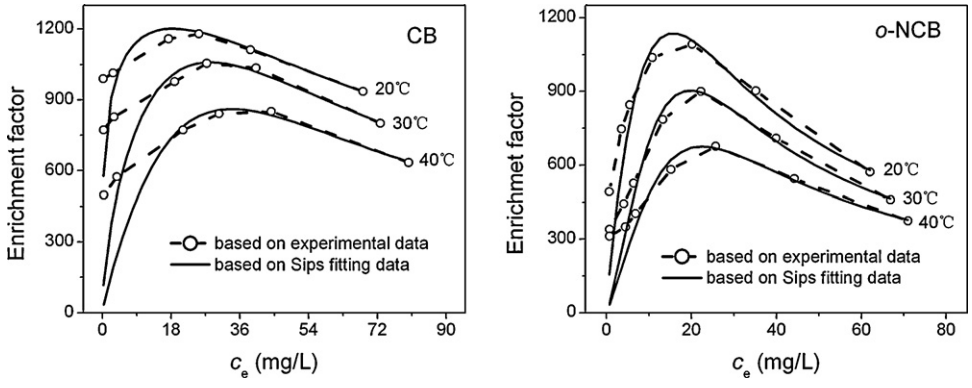

Fig. 5. EF variety of PHBBMA for CB and *o*-NCB with equilibrium concentrations at different temperatures.

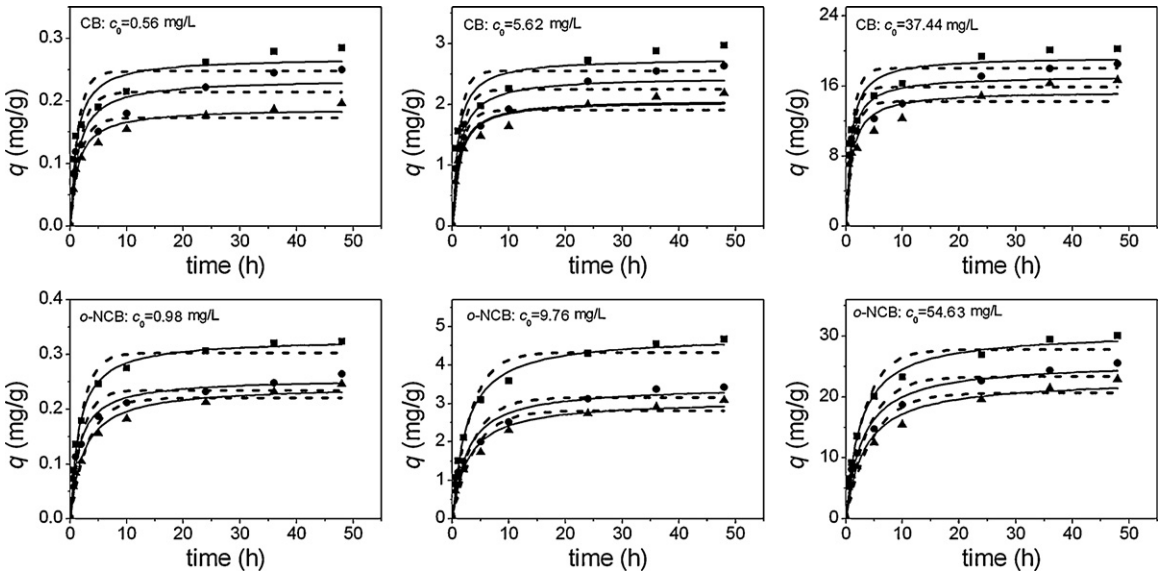

Fig. 6. Kinetics for CB and *o*-NCB on PHBBMA: experimental data at 20 °C (■), 30 °C (●) and 40 °C (▲); pseudo-first order model fitting (- - -), and pseudo-second order model fitting (—).

where k_1 (h^{-1}) is the rate constant of the first order sorption. Integrating Eq. (6) for the boundary conditions, $q = 0$ at $t = 0$ and $q = q$ at $t = t$, it gives:

$$q = q_e[1 - \exp(-k_1 t)] \quad (7)$$

The pseudo-second order model is in the form [46]:

$$\frac{dq}{dt} = k_2(q_e - q)^2 \quad (8)$$

where k_2 (g mg^{-1} h^{-1}) is the rate constant of the second order sorption. The integration of Eq. (8) with the boundary conditions, $q = 0$ at $t = 0$ and $q = q$ at $t = t$ leads to:

$$q = \frac{k_2 q_e^2 t}{1 + q_e k_2 t} \quad (9)$$

$$h_0 = k_2 q_e^2 \quad (10)$$

where h_0 (mg g^{-1} h^{-1}) is the initial sorption rate, which is obtained when t approaches to zero. The adsorption kinetics of CB and *o*-NCB on PHBBMA were fitted by Eqs. (7) and (9) employing the non-linear fitting method using the software Origin7.5 (Fig. 6). The parameters of the fitted models are presented in Table 3.

Fig. 6 shows that the pseudo-second order model could fit the experimental data better than the pseudo-first order model. The R^2 values in Table 3 also confirmed this observation for all R^2 of the second order model were higher than that of the first order model. The initial rate h_0 decreased when temperature increased because it was affected by the rate constant and the equilibrium capacity. When the temperature increased, the diffusion rate of the adsorbate molecules across the liquid film and in the internal pores of the

Table 3
Kinetic parameters for CB and *o*-NCB on PHBBMA.

Chemical c_0 (mg L^{-1})	T (°C)	Pseudo-first order model			Pseudo-second order model			
		q_e	k_1	R^2	q_e	k_2	h_0	R^2
CB								
0.56	20	0.25 (0.02)[a]	0.716 (0.200)	0.879	0.27 (0.01)	3.433 (0.942)	0.25 (0.09)	0.950
	30	0.21 (0.02)	0.574 (0.182)	0.852	0.23 (0.01)	3.084 (0.992)	0.16 (0.07)	0.933
	40	0.17 (0.01)	0.579 (0.129)	0.926	0.19 (0.01)	4.035 (0.743)	0.14 (0.03)	0.978
5.62	20	2.55 (0.17)	0.825 (0.249)	0.856	2.76 (0.14)	0.395 (0.123)	3.01 (1.25)	0.935
	30	2.25 (0.16)	0.671 (0.204)	0.860	2.46 (0.13)	0.342 (0.105)	2.07 (0.86)	0.938
	40	1.91 (0.11)	0.680 (0.174)	0.900	2.07 (0.09)	0.419 (0.101)	1.80 (0.58)	0.962
37.44	20	18.03 (1.08)	0.876 (0.235)	0.882	19.32 (0.83)	0.063 (0.017)	23.52 (8.23)	0.953
	30	15.87 (1.08)	0.889 (0.272)	0.853	17.14 (0.90)	0.068 (0.022)	19.98 (8.47)	0.932
	40	14.21 (1.04)	0.752 (0.241)	0.840	15.40 (0.88)	0.064 (0.021)	15.18 (6.85)	0.924
o-NCB								
0.98	20	0.30 (0.01)	0.484 (0.072)	0.968	0.33 (0.01)	1.978 (0.143)	0.22 (0.02)	0.997
	30	0.23 (0.01)	0.493 (0.094)	0.948	0.25 (0.01)	2.590 (0.372)	0.16 (0.03)	0.987
	40	0.22 (0.01)	0.315 (0.065)	0.943	0.24 (0.01)	1.741 (0.307)	0.10 (0.02)	0.983
9.76	20	4.33 (0.19)	0.311 (0.055)	0.960	4.76 (0.11)	0.087 (0.011)	1.97 (0.33)	0.992
	30	3.15 (0.19)	0.276 (0.066)	0.922	3.45 (0.16)	0.114 (0.026)	1.36 (0.44)	0.970
	40	2.81 (0.16)	0.261 (0.059)	0.932	3.08 (0.13)	0.120 (0.026)	1.14 (0.35)	0.974
54.63	20	27.78 (1.14)	0.307 (0.050)	0.966	30.63 (0.65)	0.013 (0.001)	12.20 (1.85)	0.994
	30	23.34 (1.25)	0.254 (0.052)	0.944	25.74 (0.94)	0.014 (0.002)	9.28 (2.33)	0.982
	40	20.67 (1.30)	0.219 (0.051)	0.927	22.88 (1.15)	0.013 (0.003)	6.80 (2.40)	0.969

[a] The standard error of the fitting value of the parameters.

adsorbent particle increased, owing to the decrease in the viscosity of the solution. In addition, changing the temperature could change the equilibrium capacity of the adsorbent for a particular adsorbate [47]. Fig. 6 also shows that the fitting effects of the kinetics are better for *o*-NCB than for CB. This result indicates that a higher reaction order than 2 fits the data of CB well, and the concentration has a greater influence on the adsorption rate of CB than of *o*-NCB.

4. Conclusions

This work showed that PHBBMA prepared with PHB by a modified double emulsion solvent evaporation technique is an effective adsorbent for enrichment of liposoluble OClCs from aqueous solution. The maximum adsorption capacity and EF were 125.99 mg g^{-1} and 1204 for CB, 39.56 mg g^{-1} and 1149 for *o*-NCB at 20 °C for 36 h, respectively, though the specific surface area of PHBBMA was only 8.45 m^2 g^{-1} at preparation conditions.

The adsorption capacity and EF have a negative correlation with the temperature, while they have a positive correlation with K_{ow}. CB has higher lipid solubility, adsorption capacity and EF than *o*-NCB. Sips adsorption isotherm and the pseudo-second order kinetic model fitted the experimental data well, and EF could be predicted accurately by the proper model.

PHBBMA can accumulate liposoluble organic compounds to realize their degradation feasibility in kinetics. Therefore, PHB, even other PHAs, can be a new biodegradable adsorption material. In the future, more chemicals will be investigated to construct mathematical relations among chemical structure, K_{ow} and EF. The optimization and modification of PHBBMA will be also studied, such as activated carbon and molecular sieve are used as carriers to increase its surface area.

Acknowledgments

This research was supported by the Hi-Tech Research and Development Program of China (No. 2006AA06Z378), the Natural Science Foundation of China (Nos. 20777018 and 20977035), the National Key Technology R&D Program of China (No. 2008BAC32B06-1), and the Science and Technology Plan Project of Guangdong Province, China (No. 2007B030103011). We also thank Prof. L. Ke for providing language help.

References

[1] M.A.Q. Khan, S.F. Khan, F. Shattari, Halogenated hydrocarbons, Encyclopedia Ecol. (2008) 1831–1843.
[2] Z.Y. Xu, Analysis on development of domestic chlor-alkali production, China Chlor-Alkali 12 (2007) 1–6 (in Chinese).
[3] Z.Y. Xu, Analysis on development of domestic chlor-alkali production, China Chlor-Alkali 1 (2008) 6–12 (in Chinese).
[4] CCAON, Products Consuming Chlorine Inventory, 2008, http://www.ccaon.com/zt/lv%5Fproduct.
[5] G. Zhang, A. Parker, A. House, B. Mai, X.D. Li, Y.H. Kang, Z.S. Wang, Sedimentary records of DDT and HCH in the Pearl River Delta, South China, Environ. Sci. Technol. 36 (2002) 3671–3677.
[6] X.M. Hua, Z.J. Shan, The production and application of pesticides and factor analysis of their pollution in environment in China, Adv. Environ. Sci. 4 (1996) 33–45 (in Chinese).
[7] X.X. Zhang, Y. Ren, M.H. He, F.Z. Zhang, H.L. Peng, C.H. Wei, W.K. Zhu, W.C. Zeng, W. Zhang, Adsorption of chlorinated organic compounds in effluents from wastewater treatment plants with powdered activated carbon, Acta Sci. Circumst. 29 (2009) 548–554 (in Chinese).
[8] Q.C. He, G.F. Cheng, Y. Ren, W.L. Pan, B.B. Huang, X.X. Zhang, C.H. Wei, Organic compounds in fine chemical wastewater, their composition analysis and topological study in biodegradability and toxixity, Chem. Ind. Eng. Prog. 28 (2009) 1080–1085 (in Chinese).
[9] X. Yang, C. Shang, J.C. Huang, DBP formation in breakpoint chlorination of wastewater, Water Res. 39 (2005) 4755–4767.
[10] S.D. Richardson, M.J. Plewa, E.D. Wagner, R. Schoeny, D.M. Demarini, Occurrence, genotoxicity, and carcinogenicity of regulated and emerging disinfection by-products in drinking water: a review and roadmap for research, Mutat. Res. 636 (2007) 178–242.
[11] H.C. Hong, Y. Liang, B.P. Han, A. Mzaumder, M.H. Wong, Modeling of trihalomethane (THM) formation via chlorination of the water from Dongjiang River (source water for Hong Kong's drinking water), Sci. Total Environ. 385 (2007) 48–54.
[12] P.H. Taylor, D. Lenoir, Chloroaromatic formation in incineration processes, Sci. Total Environ. 269 (2001) 1–24.
[13] J.J. Gao, L.H. Liu, X.R. Liu, J. Lu, H.D. Zhou, S.B. Huang, Z.J. Wang, P.A. Spear, Occurrence and distribution of organochlorine pesticides – lindane, p,p′-DDT, and heptachlor epoxide – in surface water of China, Environ. Int. 34 (2008) 1097–1103.
[14] M.C. He, Y. Sun, X.R. Li, Z.F. Yang, Distribution patterns of nitrobenzenes and polychlorinated biphenyls in water, suspended particulate matter and sediment from mid- and down-stream of the Yellow River (China), Chemosphere 65 (2006) 365–374.
[15] D.B. Janssen, J.E. Oppentocht, G.J. Poelarends, Microbial dehalogenation, Curr. Opin. Biotechnol. 12 (2001) 254–258.
[16] D.H. Pieper, Aerobic degradation of polychlorinated biphenyls, Appl. Microbiol. Biotechnol. 67 (2005) 170–191.
[17] L. Adrian, H. Görisch, Microbial transformation of chlorinated benzenes under anaerobic conditions, Res. Microbiol. 153 (2002) 131–137.
[18] S.A. Adebusoye, F.W. Picardal, M.O. Ilori, O.O. Amund, C. Fuqua, N. Grindle, Aerobic degradation of di- and trichlorobenzenes by two bacteria isolated from polluted tropical soils, Chemosphere 66 (2007) 1939–1946.
[19] B.J. Lifka, B. Ondruschka, J. Hofmann, The use of ultrasound for the degradation of pollutants in water: aquasonolysis—a review, Eng. Life Sci. 3 (2003) 253–262.
[20] A.T. Fisk, G.A. Stern, K.A. Hobson, W.J. Strachan, M.D. Loewen, R.J. Norstrom, Persistent organic pollutants (POPs) in a small, herbivorous, arctic marine zooplankton (Calanus hyperboreus): trends from April to July and the influence of lipids and trophic transfer, Mar. Pollut. Bull. 43 (2001) 93–101.
[21] D. Muir, T. Savinova, V. Savinov, L. Alexeeva, V. Potelov, V. Svetochev, Bioaccumulation of PCBs and chlorinated pesticides in seals, fishes and invertebrates from the White Sea, Russia, Sci. Total Environ. 306 (2003) 111–131.
[22] R.B. Zhou, L.Z. Zhu, Q.X. Kong, Persistent chlorinated pesticides in fish species from Qiantang River in East China, Chemosphere 68 (2007) 838–847.
[23] T.M. Sakellarides, I.K. Konstantinou, D.G. Hela, D. Lambropoulou, A. Dimou, T.A. Albanis, Accumulation profiles of persistent organochlorines in liver and fat tissues of various waterbird species from Greece, Chemosphere 63 (2006) 1392–1409.
[24] G.Q. Chen, Q. Wu, The application of polyhydroxyalkanoates as tissue engineering materials, Biomaterials 26 (2005) 6565–6578.
[25] G. Braunegg, G. Lefebvre, K.F. Genser, Polyhydroxyalkanoates, biopolyesters from renewable resources: physiological and engineering aspects, J. Biotechnol. 65 (1998) 127–161.
[26] A.A. Khardenavis, M.S. Kumar, S.N. Mudliar, T. Chakrabarti, Biotechnological conversion of agro-industrial wastewaters into biodegradable plastic, ploy β-hydroxybutyrate, Bioresour. Technol. 98 (2007) 3579–3584.
[27] D.E. Lin, Y.W. Zhang, C.H. Wei, J.R. Shen, Biodegradable plastic production by activated sludge with different carbon sources, Environ. Sci. 24 (2003) 97–101 (in Chinese).
[28] W.K. Junior, A.S. Guanabara, Methodology for product design based on the study of bionics, Mater. Des. 26 (2005) 149–155.
[29] D. Mackay, Correlation of bioconcentration factors, Environ. Sci. Technol. 16 (1982) 274–278.
[30] G.T. Wei, C.H. Wei, C.F. Wu, F.M. He, Reductive dechlorination of chlorobenzene in supercritical water catalyzed by Fe/ZrO_2, Environ. Chem. Lett., 2009, doi:10.1007/s10311-009-0204-3.
[31] B. Yan, C.H. Wei, C.S. Hu, C. Xie, J.Z. Wu, Hydrogen generation from polyvinyl alcohol-contaminated wastewater by a process of supercritical water gasification, J. Environ. Sci. 19 (2007) 1424–1429.
[32] C. Liang, Production situation and market analysis of nitrochlorobenzene, Techno-Econ. Petrochem. 23 (2007) 23–26 (in Chinese).
[33] PHYSPROP, Syracuse Research Corporation, Available from: http://www.syrres.com/esc/physdemo.htm.
[34] I.M. Abrams, J.R. Millar, A history of the origin and development of macroporous ion-exchange resins, React. Funct. Polym. 35 (1997) 7–22.
[35] R. Jayakumar, S. Nanjundan, M. Prabaharan, Metal-containing polyurethanes, poly(urethane-urea)s and poly(urethane-ether)s: a review, React. Funct. Polym. 66 (2006) 299–314.
[36] N.N. Ghosh, B. Kiskan, Y. Yagci, Polybenzoxazines—new high performance thermosetting resins: synthesis and properties, Prog. Polym. Sci. 32 (2007) 1344–1391.
[37] P.B. O'Donnell, J.W. McGinity, Preparation of microspheres by the solvent evaporation technique, Adv. Drug Deliv. Rev. 28 (1997) 25–42.
[38] Writed by S. Kindoh, T. Ishikawa, I. Abe, translated by G.X. Li, Adsorption Science, Chemical Industry Press, Beijing, 2006, pp. 40–49, 80, 161 (in Chinese).
[39] I. Langmuir, The adsorption of gases on plane surfaces of glass, mica and platinum, J. Am. Chem. Soc. 40 (1918) 1361–1403.
[40] F.A. Pavan, E.C. Lima, S.L.P. Dias, A.C. Mazzocato, Methylene blue biosorption from aqueous solutions by yellow passion fruit waste, J. Hazard. Mater. 150 (2008) 703–712.
[41] H. Freundlich, Over the adsorption in solution, Z. Phys. Chem. 57 (1906) 385–470.
[42] R. Sips, On the structure of a catalyst surface, J. Chem. Phys. 16 (1948) 490–495.

[43] R. Sennour, G. Mimane, A. Benghalem, S. Taleb, Removal of the persistent pollutant chlorobenzene by adsorption onto activated montmorillonite, Appl. Clay Sci. 43 (2009) 503–506.
[44] A. Finizio, A.D. Guardo, Estimating temperature dependence of solubility and octanol-water partition coefficient for organic compounds using RP-HPLC, Chemosphere 45 (2001) 1063–1070.
[45] S. Lagergrem, Zur theorie der sogenannten adsorption gelöster stoffe, Kungliag Svenska Vetenskapsakademiens, Handlingar 24 (1898) 1–39.
[46] Y.S. Ho, G. McKay, Pseudo-second order model for sorption processes, Proc. Biochem. 34 (1999) 451–465.
[47] S.B. Wang, H.T. Li, Kinetic modeling and mechanism of dye adsorption on unburned carbon, Dyes Pigments 72 (2007) 308–314.